Bond Graph Based Modal Representations and Model Reduction of Lumped Parameter Systems

Loucas S. Louca

University of Cyprus
Department of Mechanical and Manufacturing Engineering
75 Kallipoleos Street, Nicosia 1678, CYPRUS

E-mail: lslouca@ucy.ac.cy

ABSTRACT

Modal analysis is extensively used to study dynamic behavior of continuous and lumped parameter linear systems. More specifically, modal analysis can be used for the analysis and controller design of dynamic systems. In both cases, reduction of model size without degrading the accuracy is often required for the efficient use of the model. The reduction of modal models has been extensively studied and many reduction techniques are available. The majority of these techniques use frequency as the metric to determine the reduced model. This paper describes a new method for calculating the modal power of lumped parameter systems with the use of the bond graph representation, which is developed through a power conserving modal decomposition. This method is then used to reduce the size of the model. This technique is based on the Model Order Reduction Algorithm (MORA), which uses an energy-based metric to generate a series of proper reduced models. An illustrative example is provided to demonstrate the calculation of the modal power and the elimination of unimportant modes or modal elements using MORA.

Keywords

Modal Power, Modal Analysis, Bond Graphs, Model Reduction, Linear Systems, Energy Metrics, Proper Models.

INTRODUCTION

Modeling and simulation have yet to achieve wide utilization as commonplace engineering tools. One reason is that current modeling and simulation techniques are inadequate. A major disadvantage is that they require sophisticated users who are often not domain experts and thus lack the ability to effectively utilize the model and simulation tools to uncover the important design trade-offs. Another drawback is that models are often large and complicated, with many parameters, making the physical interpretation of the model outputs, even by domain experts, difficult. This is particularly true when "unnecessary" features are included in the model. It is the premise of this work that more effective use of modeling and simulation necessitates the need for proper models, that is, models with physically meaningful states and parameters that are of necessary but sufficient complexity to meet the engineering objective.

A variety of algorithms have been developed and implemented to help automate the production of proper models of dynamic systems. Wilson and Stein (1995) developed MODA (Model Order Deduction Algorithm) that deduces the needed system model complexity from subsystem models of variable complexity using a frequency-based metric. Additional work on deduction algorithms for generating proper models in an automate fashion has been reported by Ferris et al. (1994), Ferris and Stein (1995) and Walker et al. (1996). These algorithms have been implemented and demonstrated in a computer automated modeling environment (Stein and Louca, 1996).

In an attempt to overcome the limitations of the frequency-based metrics, Louca et al. (1997) introduced a new model reduction technique that also generates proper models. This approach uses an energy-based metric (element activity) that in general, can be applied to nonlinear systems (Louca et al., 1998; Louca, 1998), and considers the importance of all energetic elements (generalized inductance, capacitance and resistance) in the model. The contribution of each element in the model is ranked according to the energy metric under specific excitation. Elements with small contribution are eliminated in order to produce a reduced model. The element activity metric provides more flexibility from frequency-based metrics that address the issue of model complexity by the frequency content of the model (Margolis and Young, 1977). In contrast, the activity metric considers the importance of all energetic elements, and therefore, the significance of all energy elements in the model can be described. The purpose of the current paper is to apply this metric to modal representations of linear systems in order to demonstrate the ability of the activity to address modeling questions of modal analysis. The bond graph representation is used for model development and modal analysis, since it provides an easy and straightforward procedure for calculating the activity metric and later for reducing the model.

Proceedings 20th European Conference on Modelling and Simulation
Wolfgang Borutzky, Alessandra Orsoni, Richard Zobel © ECMS, 2006
ISBN 0-9553018-0-7 / ISBN 0-9553018-1-5 (CD)

This paper is organized as follows: First, background about the energy-based metric is provided, along with activity calculations for linear systems under steady state conditions. The next section presents the derivation of a bond graph representation of modal decomposition along with modal activity calculations. Then an illustrative example of a linear quarter car model is presented, in order to demonstrate the generation of reduced modal representations using the activity metric. Finally, a summary and set of conclusions are given.

BACKGROUND

The original work on the energy-based metric for model reduction (Louca et al., 1997) is briefly described here for convenience. Some extensions and applications of this idea are given by Louca and Stein, 2002; Louca et al., 1998; Louca, 1998.

The main idea behind this model reduction technique is to evaluate the "element activity" of the individual energy elements of a full system model under a stereotypic set of input and initial conditions. The activity of each energy element establishes a hierarchy for all the elements. Those below a user-defined threshold of acceptable level of activity are eliminated from the model. A reduced model is then generated and a new set of governing differential equations is derived.

The activity metric and MORA have been previously formulated for systems with nonlinearities in both the ideal element constitutive laws and junction structure. In this paper, MORA is applied to linear systems for which analytical expressions for the activity can be derived, and therefore, avoid the use of numerical time integration that could be cumbersome. The analysis is simplified even more if, in addition to the linearity assumption, the system is assumed to have a single sinusoidal excitation, and only the steady state response is examined. These assumptions are motivated from Fourier analysis where an arbitrary function can by decomposed into a series of harmonics. Using this decomposition, the activity analysis can be performed as a function of frequency in order to study the frequency dependency of reduced linear models as generated by MORA.

Linear System Element Activity

A measure of the power response of a dynamic system, which has physical meaning and a simple definition, is used to develop the modeling metric, element activity (or simply "activity"). The element activity, *A*, is defined for each energy element as:

$$A = \int_0^\tau \left| \mathcal{P}(t) \right| \cdot dt \qquad (1)$$

where $\mathcal{P}(t)$ is the element power and τ is the time over which the model has to predict the system behavior. The activity has units of energy, representing the amount of energy that flows in and out of the element over the given time τ. The energy that flows in and out of an element is a measure of how active this element is (how much energy passes through it), and consequently the quantity in Eq. (1) is termed *activity*.

The activity is calculated for each energy element based on the system response. In the case that the system is modeled using a bond graph formulation, the state equations are derived using the multiport bond graph representation (Rosenberg and Karnopp, 1983; Karnopp, et al, 1990). Also, when a single input system has linear junction structure and linear constitutive laws, which yield linear time invariant state equations, the state equations have the general form:

$$\dot{\mathbf{x}} = \mathbf{A} \cdot \mathbf{x} + \mathbf{b} \cdot u, \quad \mathbf{x}(0) = \mathbf{x}_0 \qquad (2)$$

where:

$\mathbf{A} \in \Re^{n \times n}$, $\mathbf{b} \in \Re^n$ are the constant state space matrices,

$\mathbf{x} \in \Re^n$ is the state vector, and *n* is the number of independent states,

$u \in \Re$ is the input,

$\mathbf{x}_0 \in \Re^n$ are the initial conditions of the states.

Appropriate outputs are defined in order to calculate the power of each element in the model using the constitutive law of each element. For convenience, the outputs are selected to be flow, effort, and flow for inertial, compliant, and resistive elements, respectively. The output vector for this set of variables has the form:

$$\mathbf{y} = \begin{Bmatrix} \mathbf{f}_I \\ \hdashline \mathbf{e}_C \\ \hdashline \mathbf{f}_R \end{Bmatrix} \qquad (3)$$

where $\mathbf{y} \in \Re^k$ and $\mathbf{f}_I, \mathbf{e}_C,$ and $\mathbf{f}_R$ are vectors of size $k_I, k_C,$ and k_R respectively. The variables $k_I, k_C,$ and k_R represent the number of inertial, compliant and resistive elements, respectively, and total number of energy elements in the system is $k = k_I + k_C + k_R$. For the output variables given Eq. (3) and using the multiport bond graph representation, the output equations can be written as:

$$\mathbf{y} = \mathbf{C} \cdot \mathbf{x} + \mathbf{d} \cdot u \qquad (4)$$

where $\mathbf{C} \in \Re^{k \times n}$, $\mathbf{d} \in \Re^k$ are the constant output state space matrices. Given these variables the required efforts or flows for calculating the element power, are computed from their constitutive law as shown below:

$$\begin{aligned} &\text{I:} \quad p = r_I \cdot f_I \Leftrightarrow e_I = \dot{p} = r_I \cdot \dot{f}_I \\ &\text{C:} \quad q = r_C \cdot e_C \Leftrightarrow f_C = \dot{q} = r_C \cdot \dot{e}_C \\ &\text{R:} \quad e_R = r_R \cdot f_R \end{aligned} \tag{5}$$

where r_I, r_C, r_R are known constants. A vector, $\mathbf{r}$, with all the constitutive law coefficients is introduced as shown below:

$$\mathbf{r} = \begin{Bmatrix} \mathbf{r}_I \\ \hline \mathbf{r}_C \\ \hline \mathbf{r}_R \end{Bmatrix} \tag{6}$$

where $\mathbf{r} \in \Re^k$, $\mathbf{r}_I \in \Re^{k_I}$, $\mathbf{r}_C \in \Re^{k_C}$, and $\mathbf{r}_R \in \Re^{k_R}$. This vector is used later in the analysis to produce concise expressions. Finally, the power needed for calculating the activity in Eq. (1) is computed from Eq. (5) as:

$$\begin{aligned} &\text{I:} \quad \mathcal{P}_I = e_I \cdot f = r_I \cdot \dot{f}_I \cdot f_I \\ &\text{C:} \quad \mathcal{P}_C = e_C \cdot f_C = r_C \cdot e_C \cdot \dot{e}_C \\ &\text{R:} \quad \mathcal{P}_R = e_R \cdot f_R = r_R \cdot f_R \cdot f_R \end{aligned} \tag{7}$$

Activity Index and MORA

The activity as defined in Eq. (1) is a measure of the absolute importance of an element as it represents the amount of energy that flows through the element over a given time period. In order to obtain a relative measure of the importance, the element activity is compared to a quantity that represents the "overall activity" of the system. This "overall activity" is defined as the sum of all the element activities of the system, is termed total activity (A^{Total}) and is given by:

$$A^{Total} = \sum_{i=1}^{k} A_i \tag{8}$$

where A_i is the activity of the i^{th} element given by Eq. (1). Thus a normalized measure of element importance, called the element activity index or just activity index, is defined as:

$$AI_i = \frac{A_i}{A^{Total}} = \frac{\int_0^\tau \left| \mathcal{P}_i(t) \right| \cdot dt}{\sum_{i=1}^{k} \left\{ \int_0^\tau \left| \mathcal{P}_i(t) \right| \cdot dt \right\}}, \quad i = 1,\ldots,k \tag{9}$$

The activity index, AI_i, is calculated for each element in the model and it represents the portion of the total system energy that flows through a specific element. This calculation is typically performed on the results produced by numerical integration of the system state equations. MORA then produces a reduced model by eliminating elements from the model based on their activity (Louca et al., 1997).

Single Harmonic Excitation

The time response of the outputs, $\mathbf{y}(t)$, in Eq. (3) is required in order to complete the calculation of the element power. For the purposes of this work it is assumed that the excitation is a single harmonic of frequency ω:

$$u(t) = U \cdot \sin(\omega \cdot t) \tag{10}$$

where $U \in \Re$ is the amplitude of the excitation and ω is the excitation frequency. The steady state response for the excitation in Eq. (10) is calculated using linear system analysis. The response of the output vector $\mathbf{y}$ is given by:

$$y_i(t,\omega) = U \cdot Y_i(\omega) \cdot \sin\left(\omega \cdot t + \varphi_i(\omega)\right) \tag{11}$$

where:

$\mathbf{Y}(\omega) = \left|\mathbf{G}(j \cdot \omega)\right|$, is the steady state amplitude

$\boldsymbol{\varphi}(\omega) = \sphericalangle \mathbf{G}(j \cdot \omega)$, is the steady state phase shift

$\mathbf{G}(s) = \mathbf{C} \cdot \left(s \cdot \mathbf{I} - A\right)^{-1} \cdot \mathbf{b} + \mathbf{d}$

$i = 1,\ldots,k$

The output, $y_i(t,\omega)$ in Eq. (11), is either an effort or a flow that is needed to calculate the power of each element in Eq. (7). The element power can then be used to calculate the element activity. However, in order to compute the activity, the upper bound of the integral in Eq. (1) must be determined first. For this case, the periodicity feature of the response is exploited. A periodic function repeats itself every T seconds, and therefore, a single period of this function contains the required information about the response. Thus, the upper bound of the integral is set to one period of the excitation, $T = 2\pi/\omega$.

The activity of the energy elements is calculated by substituting Eq. (11) into Eq. (7) and then by using the definition of the activity in Eq. (1). These substitutions give the steady state activity for the energy storage elements $i = 1,\ldots,k_I+k_C$:

$$\begin{aligned} A_i^{ss} &= \int_0^T \left| \frac{r_i \cdot \omega \cdot U^2 \cdot Y_i^2 \cdot \sin\left(2\left(\omega \cdot t + \varphi_i\right)\right)}{2} \right| \cdot dt \\ &\Rightarrow A_i^{ss}(\omega) = 2 \cdot r_i \cdot U^2 \cdot Y_i^2(\omega) \end{aligned} \tag{12}$$

and energy dissipation elements $i = k_I+k_C+1,\ldots,k$:

$$\begin{aligned} A_i^{ss} &= \int_0^T \left| r_i \cdot U^2 \cdot Y_i^2 \cdot \sin^2(\omega \cdot t + \varphi_i) \right| \cdot dt \\ &\Rightarrow A_i^{ss}(\omega) = \frac{\pi \cdot r_i \cdot U^2 \cdot Y_i^2(\omega)}{\omega} \end{aligned} \tag{13}$$

Next, the activity indices are calculated as defined in Eq. (9). For the activity results of energy storage elements $i = 1,\ldots,k_I+k_C$ in Eq. (12) the activity indices become:

$$AI_i^{ss}(\omega) = \frac{2 \cdot r_i \cdot Y_i^2}{2\sum_{j=1}^{k_I+k_C} r_j \cdot Y_j^2 + \frac{\pi}{\omega}\sum_{j=k_I+k_C+1}^{k} R_j \cdot Y_j^2} \qquad (14)$$

and for the energy dissipation elements $i = k_I+k_C+1,\ldots,k$ in Eq. (13) the activity indices are:

$$AI_i^{ss}(\omega) = \frac{\frac{\pi}{\omega} \cdot r_i \cdot Y_i^2}{2\sum_{j=1}^{k_I+k_C} r_j \cdot Y_j^2 + \frac{\pi}{\omega}\sum_{j=k_I+k_C+1}^{k} r_j \cdot Y_j^2} \qquad (15)$$

The input amplitude U does not appear in any of the element activity indices, as it is shown in Eq. (14) and (15), since all element activities are proportional to the square of the amplitude.

The above results for the activity index can be used by MORA to generate reduced models. The generated results are only valid for an input of a single frequency. However, for generic inputs the reduced model can still be generated using a Fourier expansion of the input into a series of harmonics. Using this decomposition, the analysis is first carried out for a single input sinusoidal excitation under steady state conditions. Then, the effects of each harmonic are superposed to get the aggregate response caused by a generic input.

POWER CONSERVING MODAL DECOMPOSITION

In order to calculate activity, the power of elements and modes must be available. These can be easily evaluated if the bond graph of the modal decomposition is available. In addition, it is necessary to have available all power variables for calculating the activity at all bonds. To satisfy these requirements, the system model is developed using the bond graph formulation and the equations are derived using the junction structure matrices (Rosenberg, 1971). In this case the state space matrices are given by:

$$\begin{aligned}\mathbf{A} &= \left(\mathbf{J}_{SS} + \mathbf{J}_{SL}\cdot\mathbf{L}\cdot\left(I-\mathbf{J}_{LL}\cdot\mathbf{L}\right)^{-1}\cdot\mathbf{J}_{LS}\right)\cdot\mathbf{S}\\ \mathbf{B} &= \mathbf{J}_{SU} + \mathbf{J}_{SL}\cdot\mathbf{L}\cdot\left(I-\mathbf{J}_{LL}\cdot\mathbf{L}\right)^{-1}\cdot\mathbf{J}_{LU}\end{aligned} \qquad (16)$$

where the junction structure matrices $\mathbf{J}_{??}$ represent the kinematic interconnections between the capacitance, inertance, resistance, and source multiports. This approach for representing the state equations has been selected in order to allow more flexibility in the analysis and generation of the modal decomposition. For example when the there is no path between the inputs and resistive elements ($J_{UL} = J_{LU}^T = 0$) the expressions can be significantly reduced.

Using the same approach the power flowing into the system is given by:

$$\begin{aligned}\mathbb{P}_{in}^{S} = u\cdot\left(\mathbf{J}_{US} + \mathbf{J}_{UL}\cdot\mathbf{L}\left(I-\mathbf{J}_{LL}\cdot\mathbf{L}\right)^{-1}\mathbf{J}_{LS}\right)\cdot\mathbf{S}\cdot\mathbf{x}\\ +u\cdot\mathbf{J}_{UL}\cdot\mathbf{L}\cdot\left(I-\mathbf{J}_{LL}\cdot\mathbf{L}\right)^{-1}\cdot\mathbf{J}_{LU}\cdot u\end{aligned} \qquad (17)$$

The power in Eq. (17) has a quadratic term in the input, u, which is must be considered when generating the modal expansion bond graph.

For building the modal expansion bond graph, the state equations in Eq. (2) are first decoupled after solving the eigenvalue problem for the state matrix A. The decoupled equations are then given by:

$$\dot{\mathbf{z}} = \mathbf{\Lambda}\cdot z + \mathbf{V}^{-1}\cdot\mathbf{b}\cdot u \qquad (18)$$

where $\mathbf{\Lambda} = diag\left(\lambda_1,\lambda_1^*,\ldots,\lambda_{n/2},\lambda_{n/2}^*\right)$ is the diagonal matrix with the eigenvalues of $\mathbf{A}$ and $\mathbf{V}$ is a square matrix that its rows are the eigenvectors of $\mathbf{A}$. The transformation between the real and modal states is given by $\mathbf{x} = \mathbf{V}\cdot\mathbf{z}$.

Given the decoupled modal equations a bond graph that has the same dynamic equations is developed as shown in Figure 1. The equations of this model are given by:

$$\dot{\mathbf{z}} = -\mathbf{L}_m\cdot\mathbf{S}_m\cdot z + \mathbf{L}_m\cdot\mathbf{t}\cdot u \qquad (19)$$

where

$\mathbf{L}_m = diag\left(R_1,R_1^*,\ldots,R_{n/2},R_{n/2}^*\right)$ is a square matrix representing the damping in the system,

$\mathbf{S}_m = diag\left(I_1,I_1^*,\ldots,I_{n/2},I_{n/2}^*\right)^{-1}$ is a square matrix representing the inertia of the system,

$\mathbf{t} = \left\{t_1,t_1^*,\ldots,t_{n/2},t_{n/2}^*\right\}^T$ is a vector representing the contribution of the input to each mode.

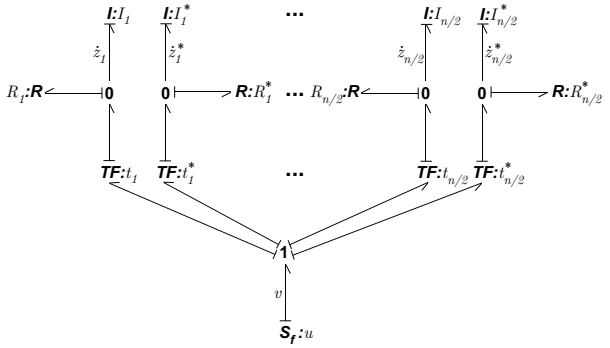

Figure 1: Complex modal decomposition

The power flowing into the modal bond graph model in Figure 1 is given by:

$$\begin{aligned} \mathcal{P}_{in}^{M} &= u \cdot \mathbf{t}^{T} \cdot \mathbf{L}_{m} \cdot \mathbf{t} \cdot u - u \cdot \mathbf{t}^{T} \cdot \mathbf{L}_{m} \cdot \mathbf{S}_{m} \cdot \mathbf{z} \\ &= u \cdot \mathbf{t}^{T} \cdot \mathbf{L}_{m} \cdot \mathbf{t} \cdot u - u \cdot \mathbf{t}^{T} \cdot \mathbf{L}_{m} \cdot \mathbf{S}_{m} \cdot \mathbf{V}^{-1} \cdot \mathbf{x} \end{aligned} \tag{20}$$

Up to now the modal bond graph in Figure 1 had a given structure but no parameters. This can be accomplished by enforcing the dynamic equations in Eq. (18) and (19) to be the same, and the power flowing into the two models as given by Eq. (17) and (20) to be equal. These conditions provide enough equations to calculate the missing parameters of the modal bond graph, and they are given by:

$$\begin{aligned} &\mathbf{t}^{T} = \left(\mathbf{J}_{US} + \mathbf{J}_{UL} \cdot \mathbf{L} \left(I - \mathbf{J}_{LL} \mathbf{L} \right)^{-1} \mathbf{J}_{LS} \right) \cdot \mathbf{S} \cdot \mathbf{V} \cdot \mathbf{\Lambda}^{-1} \\ &\mathbf{V}^{-1} \cdot \mathbf{b} = \mathbf{L}_{m} \cdot \mathbf{t} \\ &\mathbf{\Lambda} = -\mathbf{L}_{m} \cdot \mathbf{S}_{m} \end{aligned} \tag{21}$$

The model in Figure 1 has complex states and parameters, which need to be transformed into real modal states and parameters. This step is necessary in order to be able to perform the reduction and finally obtain a reduced model with real states. The transformation is depicted in Figure 2 where the i[th] mode of the system shown in the complex representation and its equivalent real realization. The parameters of the real modal bond graph are calculated by enforcing the same dynamics and power flow between the real and complex bond graphs. These leads to the following expressions for the parameters:

$$\begin{aligned} k_{i} &= \frac{1}{\left\| \lambda_{i} \right\|^{2}} = \frac{1}{\left(real\left(\lambda_{i} \right)^{2} + imag\left(\lambda_{i} \right)^{2} \right)} \\ b_{i} &= -2 \cdot real\left(\lambda_{i} \right) \\ f_{i} &= \sqrt{\frac{-m_{i} \cdot t_{i}^{2} \cdot R_{i} \cdot \lambda_{i} \cdot \left(\lambda_{i} - \lambda_{i}^{*} \right)}{-\left(b_{i} + m_{i} \cdot \lambda_{i}^{*} \right) \left(k_{i} + b_{i} \cdot \lambda_{i} \right)}}, \qquad \left(m_{i} = 1 \right) \end{aligned} \tag{22}$$

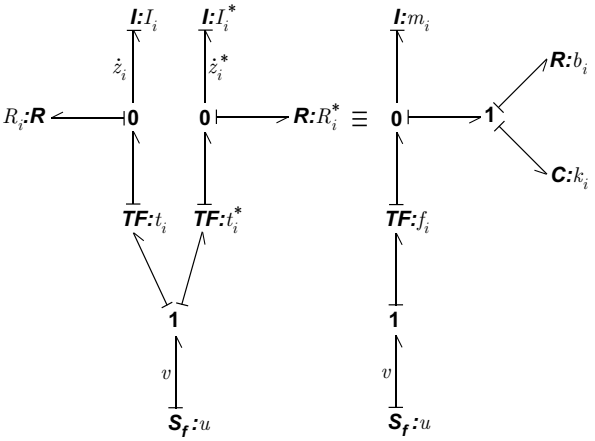

Figure 2: Complex and real modes

The equivalent real bond graph can only be calculated in the case of proportional damping. In the general non-proportional case the modes cannot be completely decoupled and therefore the decoupled bond graph in Figure 2 is not realizable.

With the above modal representation the activity analysis can be performed as described above in the previous section. The activity can be calculated for either the mode or the individual modal components. This gives as the flexibility to eliminate a complete mode or individual components of the mode (I, C, R).

ILLUSTRATIVE EXAMPLE

A quarter car model is selected as the linear system to apply MORA and modal activity. The modal decomposition model can be used to obtain reduced models as function of the excitation frequency. This model is chosen because it has been extensively used in the automotive literature and the frequency dependent properties of the system are well understood. The model consists of the sprung mass, namely, the major mass supported by the suspension, and the unsprung mass, which includes the wheel and axle masses supported by the tire. The suspension is modeled as a spring and a damper in parallel, which are connected to the unsprung mass. The tire is also modeled as a spring and a damper in parallel, which transfer the road force to the unsprung mass (wheel hub). The input to the system is the road profile that prescribes a velocity, $V_r\left(t\right)$, to the contact point of the tire with the road. The system is composed of six ideal energy elements described by an equal number of parameters. The bond graph model of the system is depicted in Figure 3 and the parameters representing a medium size passenger car are given in the Appendix. Note that the parameters satisfy the condition for proportional damping in order to be able to develop the real bond graph representation of the modal decomposition.

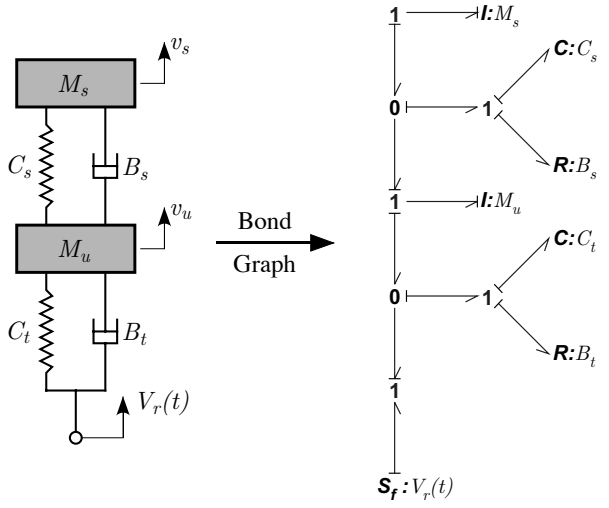

Figure 3: Full Quarter Car Model

The real bond graph representation of the modal expansion is first developed according the procedure presented in the previous section. The model has four states ($n = 4$), and therefore, the modal expansion consists of two modes that for the given set of parameters are underdamped. The modal parameters as calculated by Eq. (22) are given in Table 1 and the modal bond graph depicted in Figure 4.

Table 1: Modal parameters

Mode	m	b	k	f
1	1	0.5117	63.939	16.531
2	1	46.55	5816.6	5.5077

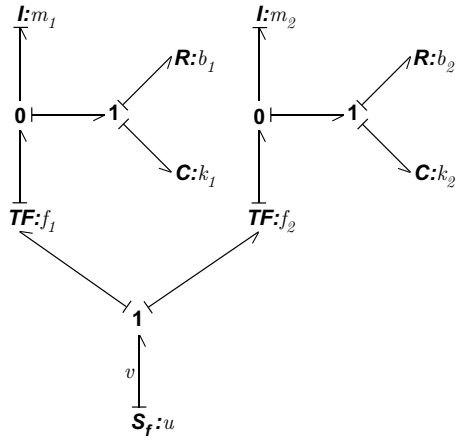

Figure 4: Modal expansion bond graph

The modal bond graph can be used to calculate the modal power and activity. The modal power is the power flowing through the transformers (f_i), which is distributed into the model elements (m_i, c_i, b_i). Using Eq. (1), the activities are calculated as a function of the road frequency. The road frequency is varied from 0.1 *rad/s* to 10000 *rad/s*, which includes all the frequencies well below and above the low (8 *rad/s*) and high (76 *rad/s*) system natural frequencies, respectively. The element activities and activity indices for the two modes are shown in Figure 5. The 1st mode (low frequency) dominates response with about 90% activity for the low range of the excitation, while the roles are reversed for the high range of frequencies where the 2nd mode (high frequency) is dominating. According to the activity analysis both modes are important and should be retained in the model except around the first resonance. The activity index of the second mode around the first resonance is very small and with a threshold of 99% MORA will produce a reduced model that includes only the first mode.

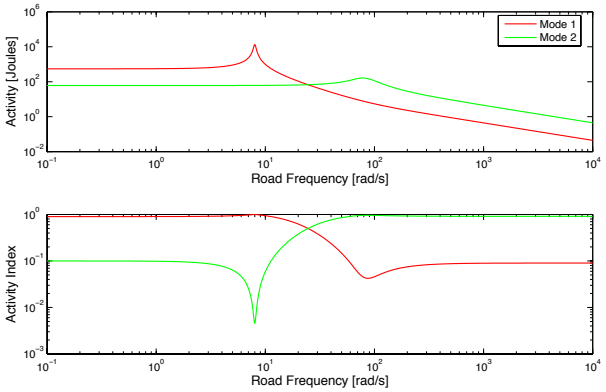

Figure 5: Activity and Activity Indices of modes

A more detailed analysis can be carried out by considering the activity of individual modal elements rather than the whole mode. The element activities are calculated using Eq. (12)-(15) and their frequency dependency is shown in Figure 6. At low frequencies the most active elements are the two modal masses. These elements handle the bulk of the energy flow induced into the system by the input. As the road frequency increases the activity of all the elements increases, and finally at the first resonance the modal elements of the first mode are the most active. The second mode elements have very small activity since most of the energy flow is handled by the first mode. The reverse is observed around the second resonance with second mode elements having the highest activities. As the frequency continues to increase, the activity of elements drops except the two modal resistances for which the activity reaches a steady state value.

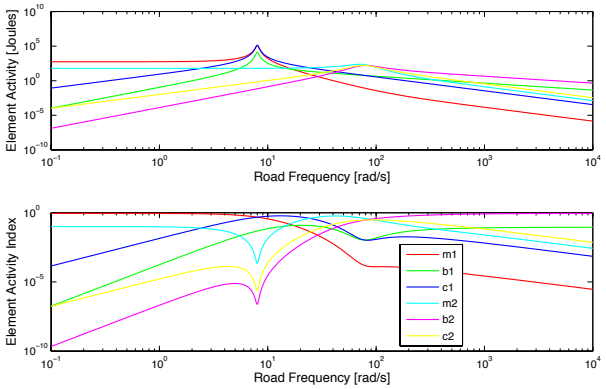

Figure 6: Modal elements activity analysis

MORA is then applied to generate a series of reduced models. Based on a 99% activity threshold (arbitrary threshold), the model complexity is determined as a function of the input road frequency. The first plot in Figure 7 shows the range of frequencies over which each element is included in the reduced model according to MORA. The y-axis represents each element, where the thick line defines the range of frequencies, over which the element should be included,

while no line implies the range of frequencies over which the element could be removed. The second plot shows the number of elements included in the reduced model and the third plot the amount of activity maintained in the reduced model.

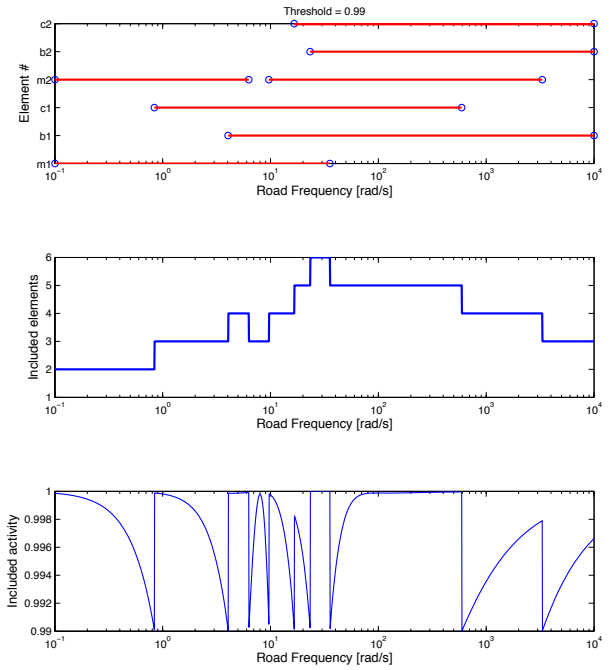

Figure 7: Included Elements, Threshold = 99%

As shown in Figure 7, a low frequency excitation requires only the rigid body model with the two modal masses as the only elements included in the reduced model. As the frequency increases, the first mode stiffness must also be included. Just before the first natural frequency, the modal elements of the second mode are eliminated and the reduced model includes only the first mode elements. This agrees with the activity analysis performed for the complete mode in Figure 5. For high frequencies the modal resistances have the highest activities and they are the only elements included along with the stiffness of the second mode.

SUMMARY AND CONCLUSIONS

A previously developed concept, an energy-based modeling metric called activity, is applied to the modal expansion of linear systems to compare model complexity as a function of frequency. It is shown that when considering the sinusoidal steady state response, the derivation of analytical expressions for the activity as function of the input frequency is possible. It is also shown that the activity varies with the frequency content of the excitation. Thus, a series of models can be generated by a previously published algorithm, MORA, which is based on the activity metric. The importance of individual modal elements, in contrast with a complete mode, can be addressed and lead to a significant reduction in model size. The benefits from this reduction are twofold. First the reduced size of the model should result in an equivalent reduction in computational cost. Second, the identification of low activity elements, and thus unimportant, reduces the development time since for these elements less accurate parameters can be used.

The results of this paper provide more insight into the nature of the reduced ordered models produced by MORA, and therefore, demonstrate that MORA is an even more useful tool than previously realized for the production of proper models of nonlinear systems. Also, a new methodology for addressing the importance of modes in modal decomposition has been developed. This methodology can handle complete modes as well as individual modal elements.

ACKNOWLEDGMENT

The author gratefully acknowledges the support of this work by the Marie Curie International Reintegration Grant (MIRG-CT-2005-022219).

REFERENCES

Ferris, J.B., and J.L. Stein, 1995. "Development of Proper Models of Hybrid Systems: A Bond Graph Formulation." *Proceedings of the 1995 International Conference on Bond Graph Modeling*, pp. 43-48, January, Las Vegas, NV. Published by SCS, ISBN 1-56555-037-4, San Diego, CA.

Ferris, J.B., J.L. Stein, and M.M. Bernitsas, 1994. "Development of Proper Models of Hybrid Systems." *Proceedings of the 1994 ASME International Mechanical Engineering Congress and Exposition - Dynamic Systems and Control Division, Symposium on Automated Modeling: Model Synthesis Algorithms*, pp. 629 - 636, November, Chicago, IL. Published by ASME, Book No. G0909B, New York, NY.

Karnopp, D.C., D.L. Margolis, and R.C. Rosenberg, 1990. *System Dynamics: A Unified Approach*. Wiley-Interscience, New York, NY.

Louca, L.S., J.L. Stein, G.M. Hulbert, and J.K. Sprague, 1997. "Proper Model Generation: An Energy-Based Methodology." *Proceedings of the 1997 International Conference on Bond Graph Modeling*, pp. 44-49, Phoenix, AZ. Published by SCS, ISBN 1-56555-103-6, San Diego, CA.

Louca, L.S. and J.L. Stein, 2002. "Ideal Physical Element Representation from Reduced Bond Graphs". *Journal of Systems and Control Engineering: Special Issue on Bond Graphs*, Vol. 216, No. 1, pp. 73-83. Published by the Professional Engineering Publishing, ISSN 0959-6518, Suffolk, United Kingdom.

Louca, L.S., J.L. Stein and G.M. Hulbert, 1998. "A Physical-Based Model Reduction Metric with an Application to Vehicle Dynamics." *The 4th IFAC Nonlinear Control Systems Design Symposium (NOLCOS 98)*. Enschede, The Netherlands.

Louca, L.S., 1998. *An Energy-Based Model Reduction Methodology For Automated Modeling*. Ph.D. Thesis. The University of Michigan, Ann Arbor, MI.

Margolis, D.L., and G.E. Young, 1977. "Reduction of Models of Large Scale Lumped Structures Using Normal Modes and Bond Graphs." *Journal of the Franklin Institute*, vol. 304, No. 1, pp. 65-79.

Rosenberg, R.C., 1971. "State-Space Formulation for Bond Graph Models of Multiport Systems." *Transactions of the ASME, Journal of Dynamic Systems, Measurement, and Control*, Vol. 93, pp. 36-40. Published by ASME, New York, NY.

Rosenberg, R.C., and D.C. Karnopp, 1983. *Introduction to Physical System Dynamics*. McGraw-Hill, New York, NY.

Stein, J.L. and L.S. Louca, 1996. "A Template-Based Modeling Approach for System Design: Theory and Implementation." *TRANSACTIONS of the Society for Computer Simulation International*. Published by SCS, ISSN 0740-6797/96, San Diego, CA.

Stein J.L and Wilson, B.H., 1995. "An Algorithm for Obtaining Proper Models of Distributed and Discrete Systems". *Transactions of the ASME: Journal of Dynamic Systems Measurement and Control*, Vol. 117, No. 4, pp. 534-540. Published by ASME, ISSN 0022-0434, New York, NY

Wilson, B.H. and J.L. Stein, 1995. "An Algorithm for Obtaining Proper Models of Distributed and Discrete Systems." *Transactions of the ASME, Journal of Dynamic Systems, Measurement, and Control*, Vol. 117, No. 4, pp. 534-540. Published by ASME, New York, NY.

APPENDIX – VEHICLE PARAMETERS

Sprung Mass, M_s	r_1 = 267 *kg*
Suspension Stiffness, K_s	r_3 = 18,742 *N/m*
Suspension Damping, B_s	r_5 = 150 *N·s/m*
Unsprung Mass, M_u	r_2 = 36.6 *kg*
Tire Stiffness, K_t	r_4 = 193,915 *N/m*
Tire Damping, B_t	r_6 = 1,552 *N·s/m*